Sol–gel synthesis and characterization of $Ba_{(1−x)}Sr_xTiO_3$ ceramics

Wei Li, Zhijun Xu*, Ruiqing Chu, Peng Fu, Jigong Hao

College of Materials Science and Engineering, Liaocheng University, Liaocheng, 252059, PR China

ABSTRACT

$Ba_{(1−x)}Sr_xTiO_3$ ($x = 0$, 0.1, 0.2, 0.3) nanopowders were synthesized from alkoxide solution precursor by sol–gel process. The $Ba_{(1−x)}Sr_xTiO_3$ powders calcined at 800 °C for 2 h were maintained in cubic phase and the cell parameters were in the range of 4.0282–3.9786. The effects of Sr doping and sintering temperature on structure and dielectric characteristics of the $Ba_{(1−x)}Sr_xTiO_3$ ceramics were investigated. The increase of Sr content in the $Ba_{(1−x)}Sr_xTiO_3$ ceramics causes the inhibition of grain growth and downward shift of Curie temperature (T_c). The T_c shift rate is 2.5 °C/mol% with increasing Sr content. At T_c, the dielectric constants of $Ba_{(1−x)}Sr_xTiO_3$ ceramics increase with the increasing of sintering temperature, and the highest permittivity (7032) is obtained for $x = 0.1$ sample sintered at 1400 °C.

© 2010 Elsevier B.V. All rights reserved.

1. Introduction

Barium titanate has been extensively employed in several industrial applications, including dynamic random access memory (DRAM) capacitor, microwave filters, infrared detectors and dielectric phase shifters, due to their excellent ferroelectric, dielectric, piezoelectric and pyroelectric properties [1–8]. For the ABO_3 perovskite, different A-site and B-site dopants (where A = Ca, Sr, La; B = Nb, Ta, Zr) are used to modify the electrical properties of $BaTiO_3$ based compositions [6–9].

Recently, barium strontium titanate (BST) has attracted much attention because of its strong dielectric nonlinearity under bias electric field and linearly adjustable Curie temperature with the strontium content over a wide temperature range [9–11]. The desired properties make BST a promising candidate material for tunable microwave dielectric devices [12,13]. Ferroelectric and dielectric properties of BST ceramics are strongly dependent on the sintering conditions, grain size, porosity, doping amount and structural defects. It is implied that proper doping and sintering conditions may be a promising way to improve the dielectric properties of BST ceramics [14–16]. Conventional solid-state reaction is not suitable for preparing BST powders with high performance, due to their high calcine temperature (900–1100 °C) [17–19]. Hence, it is necessary and important to adopt other methods to synthesize BST powders with desired characteristics. Recently, the sol–gel process has been intensively studied because it is very effective at producing ceramic powders of high purity, small size and good uniformity at relatively low sintering temperature [5,20].

In this work, $Ba_{(1−x)}Sr_xTiO_3$ ($x = 0$, $x = 0.1$, 0.2, 0.3) powder and ceramics were prepared by a sol–gel method. The effects of Sr content and sintering temperature on grain size and dielectric properties were investigated.

2. Experimental

$Ba_{(1−x)}Sr_xTiO_3$ ($x = 0$, 0.1, 0.2, 0.3) powders were synthesized by the sol–gel process using tetrabutyl titanate $Ti(OC_4H_9)_4$ (99.0%), barium acetate $Ba(CH_3COO)_2$ (99.0%) and strontium acetate $Sr(CH_3COO)_2$ (99.0%) as starting materials. The synthesis procedure is as follows: firstly, the mixed solution (A) of $Ti(OC_4H_9)_4$, ethanol and glacial acetic acid was obtained by stirring at room temperature. Then, $Ba(CH_3COO)_2$ aqueous solution (B) was prepared by dissolving $Ba(CH_3COO)_2$ and $Sr(CH_3COO)_2$ in 36% acetic acid. For preparing BST precursor, solution (B) was added into the solution (A) with stirring vigorously for 1 h to form a stoichiometric ratio sol. 4 h later, a clear gel was formed at room temperature. The xerogels were obtained by drying precursor in an oven at 120 °C for 8 h and then was ground and heat-treated to obtain the crystalline $BaTiO_3$ powder. For all samples, the calcination treatment was performed at 800 °C for 2 h. After mixed with PVB, the powders were compressed into discs of 10 mm in diameter and 1 mm in thickness, followed by sintering at various temperatures for 2 h. After polishing, silver paste was coated on both sides of the sintered discs and then was fired at 740 °C for 20 min to form electrodes. The ceramics were poled under a dc field of 1.5 kV/mm at 25 °C in a silicon oil bath for 15 min. The crystal structures of $BaTiO_3$ powders and ceramics were determined by X-ray diffraction (XRD) using a Cu $K\alpha$ radiation ($\lambda = 1.54178$ Å) (D8 Advance, Bruker Inc., Germany). The microstructures of powders and ceramics were characterized using a scanning electron microscope (SEM) (JSM-5900, Japan). The dielectric properties were measured by precision impedance analyzer (4294A Agilent Inc., America) controlled by a computer at 100 kHz with the testing temperature ranged from ambient temperature to 150 °C.

3. Results and discussion

All of the X-ray diffraction (XRD) patterns of the $Ba_{(1−x)}Sr_xTiO_3$ powders calcined at 800 °C have pure perovskite structure, as shown in Fig. 1. It indicates that Sr^{2+} has diffused into the $BaTiO_3$

* Corresponding author. Tel.: +86 6358230923; fax: +86 6358230923.
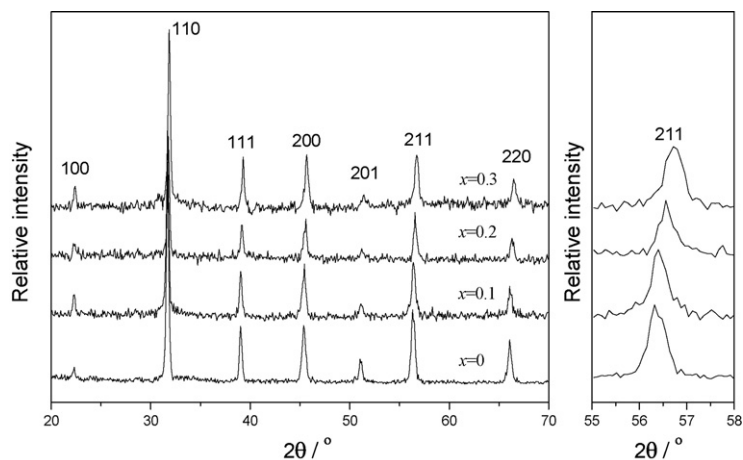*E-mail addresses:* zhjxu@lcu.edu.cn, liwei_727@yahoo.cn (Z. Xu).

Fig. 1. XRD patterns of the $Ba_{(1-x)}Sr_xTiO_3$ powders calcined at 800 °C.

lattices to form a homologous solid solution at relative low calcined temperature. The reflections (2 1 1) shift obviously towards high angles by increasing the Sr content, implying that the incorporation of Sr^{2+} into $BaTiO_3$ lattice has taken place. For clear peak shift of BST according to the Sr content, the reflections (2 1 1) are presented separately. The lattice parameters for various unit cells of BST were calculated from XRD results, as shown in Fig. 2. The value of unit cell parameter decreases with increasing the mole ratios of Sr to Ba components. The results should be attributed to the fact that the smaller strontium ion Sr^{2+} substitutes for the barium ion Ba^{2+} in the lattice and decreases the distortion of the unit cell [21].

Fig. 3 shows the SEM micrographs of $Ba_{(1-x)}Sr_xTiO_3$ ceramics sintered at different temperatures($T_{s1} = 1300$ °C, $T_{s2} = 1350$ °C, and $T_{s3} = 1400$ °C). It can be seen that the structures of $Ba_{(1-x)}Sr_xTiO_3$ ceramics vary with the mole ratios of Sr to Ba components. The grain size of $Ba_{(1-x)}Sr_xTiO_3$ ceramics sintered at T_{s1} are under 10 μm and anomalous. With the increase of the Sr content, the grain growth is restrained obviously and the grain size becomes small. There is a singular grain growth for all the ceramics after sintered at T_{s2}. The average grain size, which belongs to coarse-grained category [7], is
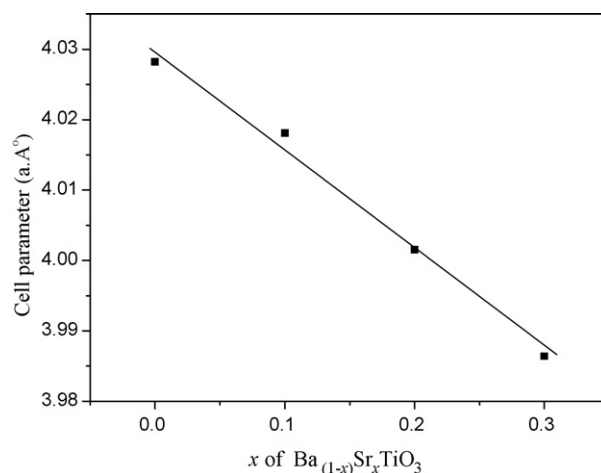

Fig. 2. Plot of Cell parameter variations with x for the $Ba_{(1-x)}Sr_xTiO_3$ ceramics.

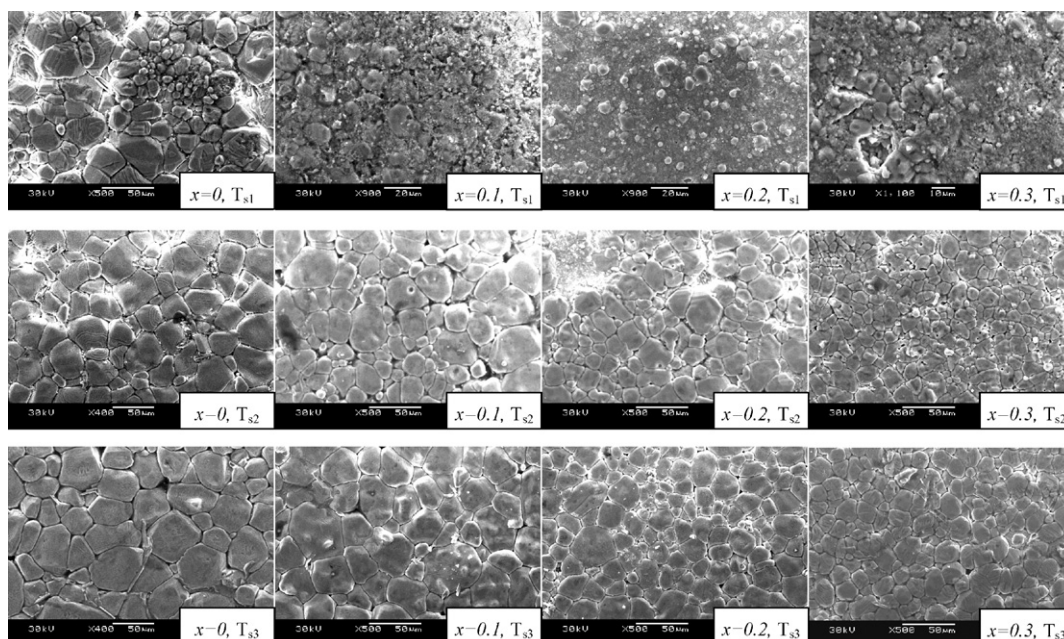**Fig. 3.** SEM micrographs of the $Ba_{(1-x)}Sr_xTiO_3$ ceramics sintered at T_{s1}, T_{s2}, and T_{s3}.

40 μm, 20 μm, 30 μm and 10 μm for the Ba$_{(1-x)}$Sr$_x$TiO$_3$ ceramics at $x = 0$, $x = 0.01$, $x = 0.02$ and $x = 0.03$, respectively. With the sintered temperature rising to T_{s3}, the grain size of the Ba$_{(1-x)}$Sr$_x$TiO$_3$ ceramics at $x = 0$, $x = 0.01$, $x = 0.02$ and $x = 0.03$ increase to 50 μm, 50 μm, 40 μm and 30 μm, respectively. At each specific sintering temperature, the grain size decreases with increasing mole ratios of Sr to Ba components. It can be confirmed that the substitution of Ba^{2+} with Sr^{2+} leads to an evident inhibition of grain growth for Ba$_{(1-x)}$Sr$_x$TiO$_3$ ceramics.

Fig. 4 shows the dielectric constant and dielectric loss of the poled Ba$_{(1-x)}$Sr$_x$TiO$_3$ ceramics sintered at T_{s1}, T_{s2} and T_{s3}, respectively, as a function of temperature at 100 kHz. The maximum

dielectric constant occurs around Curie temperature (T_c) and the T_c is found to shift downwards with the increase of Sr content. In order to quantify this behavior, Curie temperature variations as a function of Sr content was plotted in Fig. 5. It can be seen that, for Ba$_{(1-x)}$Sr$_x$TiO$_3$ ceramics, T_c decreases by a factor of 2.5 °C/mol% with increasing Sr content for each sintered temperature. Such a decrease in Curie temperature results from the substitution of smaller Sr^{2+} ions with larger Ba^{2+} ions that lead to the constriction in oxygen octahedron and compressive stress on adjacent lattices [22]. The maximum dielectric constants of the Ba$_{(1-x)}$Sr$_x$TiO$_3$ ceramics as a function of sintered temperature were plotted in Fig. 5. It is observed that the maximum dielectric constants of
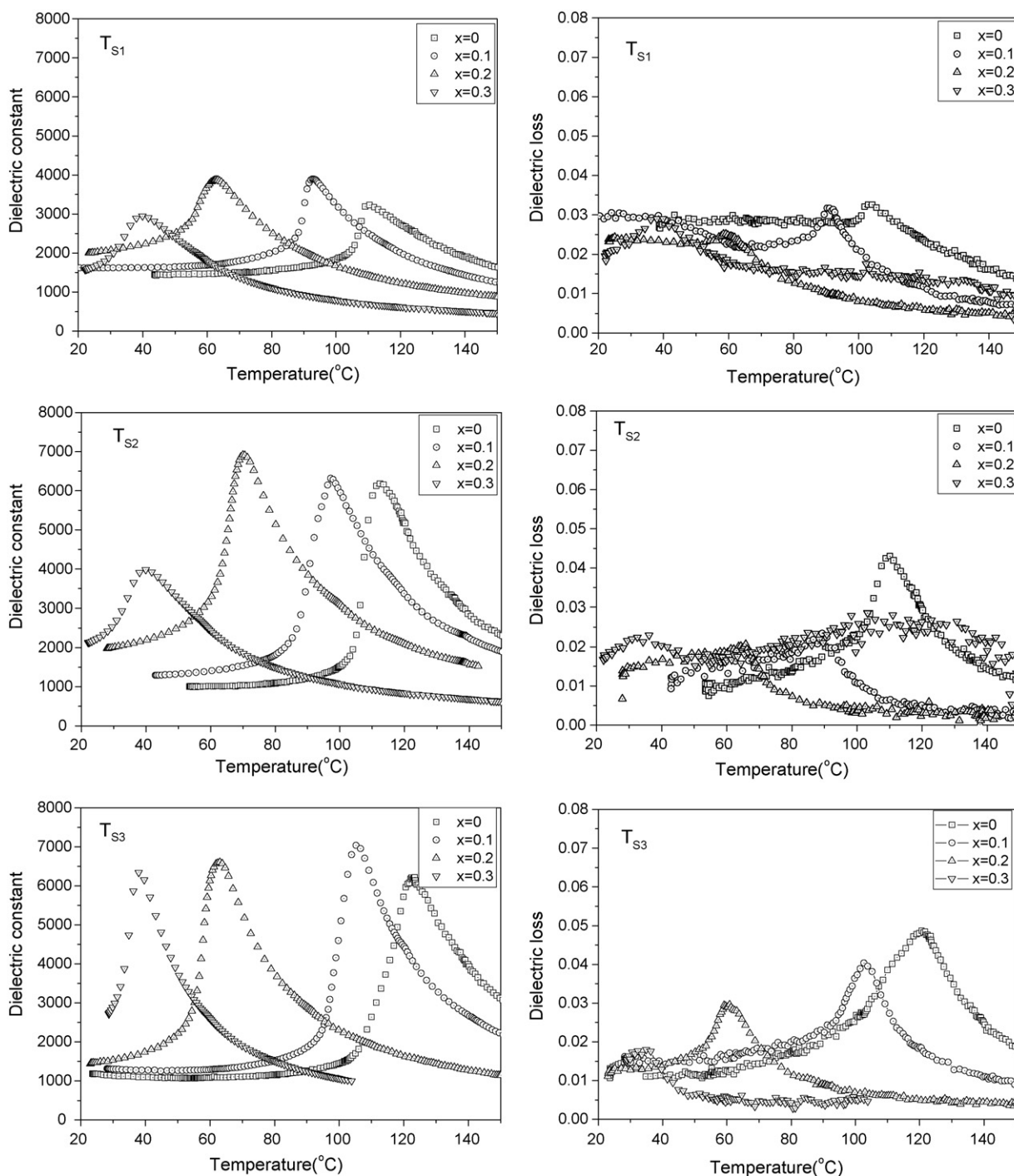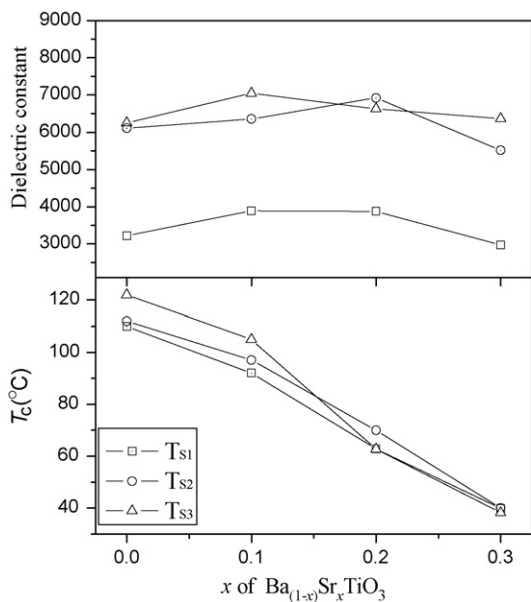

Fig. 4. Temperature dependence of the dielectric constant and dielectric loss for the Ba$_{(1-x)}$Sr$_x$TiO$_3$ ceramics sintered at T_{s1}, T_{s2}, and T_{s3}.

Fig. 5. Variations of Curie temperature and maximum dielectric constant with x for Ba$_{(1-x)}$Sr$_x$TiO$_3$ ceramics sintered at T_{s1}, T_{s2}, and T_{s3}.

the Ba$_{(1-x)}$Sr$_x$TiO$_3$ ceramics sintered at T_{s1} are at the range of 3000–4000. When the sintering temperature reaches up to T_{s2}, the dielectric constants of Ba$_{(1-x)}$Sr$_x$TiO$_3$ ceramics at $x = 0$, $x = 0.01$, $x = 0.02$ and $x = 0.03$ are 6107, 6359, 6925 and 5515, respectively. The dielectric constants of Ba$_{(1-x)}$Sr$_x$TiO$_3$ ceramics sintered at T_{s3} are 6254, 7032, 6626 and 6363, according to the sample of $x = 0$, $x = 0.01$, $x = 0.02$ and $x = 0.03$, respectively. The maximum dielectric constants increase obviously with increasing sintered temperature. Both of the maximum value 6925 for $x = 0.02$ sample sintered at T_{s2} and 7032 for $x = 0.01$ sample sintered at T_{s3} are higher than 3000 of Ba$_{0.68}$Sr$_{0.32}$TiO$_3$ [17] and 4100 of Ba$_{0.8}$Sr$_{0.2}$TiO$_3$ [19]. The increasing of dielectric constants is consistent with the grain growth of Ba$_{(1-x)}$Sr$_x$TiO$_3$ ceramics, according to the SEM results in Fig. 3. When the grain size is under 10 μm, the dielectric constant is as low as 3000–4000. As grain size grows to about 50 μm, the dielectric constants increase to 6000–7032. The sample of $x = 0.01$ sintered at T_{s3} with the maximum dielectric constant (7032), exhibits the biggest and most homogeneous grain size. It can be concluded that the grain size has great effect on the dielectric constants of the Ba$_{(1-x)}$Sr$_x$TiO$_3$ ceramics.

4. Conclusions

The Ba$_{(1-x)}$Sr$_x$TiO$_3$ ceramics were prepared by sol–gel process. Grain growth is controlled efficiently and Curie temperatures (T_c) decrease with the increasing Sr content. The Curie point shift rate is 2.5 °C/mol% with increasing Sr content. The grain size and dielectric constants at Curie point increase with the increase of sintered temperature.

Acknowledgments

References

[1] O.P. Thakur, P. Chandra, A.R. James, J. Alloys Compd. 470 (2009) 548–551.
[2] H.I. Hsiang, C.S. Hsi, C.C. Huang, S.L. Fu, J. Alloys Compd. 459 (2008) 307–310.
[3] Z.G. Hu, Y.W. Li, M. Zhu, Z.Q. Zhu, J.H. Chu, Phys. Lett. A 372 (2008) 4521–4526.
[4] S.F. Wang, Y.R. Wang, Y.C. Wu, Y.J. Liu, J. Alloys Compd. 480 (2009) 449–504.
[5] M. Cernea, E. Andronescu, R. Radu, F. Fochi, C. Galassi, J. Alloys Compd. 490 (2010) 690–694.
[6] H.Y. Tian, Y. Wang, J. Miao, H.L.W. Chan, C.L. Choy, J. Alloys Compd. 431 (2007) 197–202.
[7] J.Y. Chen, Y.W. Tseng, C.L. Huang, J. Alloys Compd. 494 (2010) 205–209.
[8] F. Boujelben, F. Bahri, C. Bouday, A. Maalej, H. Khemakhem, A. Simon, M. Maglione, J. Alloys Compd. 481 (2009) 559–562.
[9] Q. Xu, X.F. Zhang, Y.H. Huang, W. Chen, H.X. Liu, M. Chen, B.H. Kim, J. Alloys Compd. 488 (2009) 448–453.
[10] L.N. Su, P. Liu, Y. He, J.P. Zhou, L. Cao, C. Liu, H.W. Zhang, J. Alloys Compd. 494 (2010) 330–335.
[11] D. Gulwade, P. Gopalan, Solid State Commun. 146 (2008) 340–344.
[12] P.S. Sahoo, A. Panigrahi, S.K. Patri, R.N.P. Choudhary, J. Alloys Compd. 484 (2009) 832–836.
[13] X. Chou, J. Zhai, X. Yao, Mater. Chem. Phys. 109 (2008) 125–130.
[14] S. Bhaskar Reddy, K. Prasad Rao, M.S. Ramachandra Rao, J. Alloys Compd. 481 (2009) 692–696.
[15] S.B. Deshpande, Y.B. Khollam, S.V. Bhoraskar, S.K. Date, S.R. Sainkar, H.S. Potdar, Mater. Lett. 59 (2005) 293–296.
[16] Q. Xu, X.F. Zhang, Y.H. Huang, W. Chen, H.X. Liu, M. Chen, B.H. Kim, J. Alloys Compd. 485 (2009) L16–L20.
[17] Y.L. Li, Y.F. Qu, Mater. Res. Bull. 44 (2009) 82–85.
[18] X.S. Wang, L.L. Zhang, H. Liu, J.W. Zhai, X. Yao, Mater. Chem. Phys. 112 (2008) 675–678.
[19] N.C. Pramanik, N. Anisha, P.A. Abraham, N. Rani Panicker, J. Alloys Compd. 476 (2009) 524–528.
[20] B. Cui, P. Yu, X. Wang, J. Alloys Compd. 459 (2008) 589–593.
[21] D.S. Jung, S.K. Hong, J.S. Cho, Y.C. Kang, Mater. Res. Bull. 43 (2008) 1789–1799.
[22] V. Buscaglia, M.T. Buscaglia, M. Viviani, J. Eur. Ceram. Soc. 26 (2006) 2889–2898.